Larhyss Journal, ISSN 1112-3680, n°61, March 2025, pp. 371-399

UNEXPECTED FLOODING IN MERSA MATRUH, EGYPT INVESTIGATING CAUSES, HYDROLOGICAL ANALYSIS, AND FLOOD RISK ASSESSMENT

EZZ H. [1,2]

[1] Civil Engineering, Department, National Research Centre, Egypt
[2] Al Madinah High Institute for Engineering and Technology, Egypt

ezz.hisham@gmail.com

Research Article – Available at http://larhyss.net/ojs/index.php/larhyss/index
Received May 11, 2024, Received in revised form February 21, 2025, Accepted February 23, 2025

ABSTRACT

This study investigates the unexpected flood event that is reported in Mersa Matruh, Egypt, in October 2023, using hydrological modeling techniques. Despite the recorded precipitation depth being lower than that of a 2-year return period storm, the area experienced significant flooding. To address this anomaly, the study applied the Soil Conservation Service Curve Number (SCS-CN) method, calculating surface runoff based on preprocessed land use, soil, and hydrological data. Using the HEC-HMS software, runoff and flood hydrographs are simulated for a 50-year return period precipitation event. The analysis showed significant variation in peak runoff discharge across the five basins, with peak values ranging from 103.7 m^3/s to 782.3 m^3/s. A flood hazard map is developed to identify high-risk flood zones, highlighting the most vulnerable areas for future flooding events. These findings suggest that factors such as insufficient drainage infrastructure, malfunctioning flood protection measures, and topographical influences may have exacerbated the flooding. The results provide crucial insights into the hydrological processes contributing to the October 2023 flood and offer valuable data for developing effective flood risk management and mitigation strategies in the region.

Keywords: Flood analysis, DEM, Remote sensing, Spatial analyst, Flood hazard map.

INTRODUCTION

Currently, the world is grappling with the increasing frequency and severity of disasters driven by climate change (Torresan et al., 2008; Bouguerra and Benslimane, 2017). Climate-driven disasters have profound impacts on ecosystems, water resources (Nichan and Khelil, 2015; Remini, 2020; Assemian et al., 2021; Nakou et al., 2023; Chadee et al., 2023), human health, and the global economy (Aroua, 2018). Addressing these disasters requires urgent action in the form of climate adaptation strategies, sustainable resource

management (Argaz, 2018; Aroua, 2023), and global cooperation to mitigate the adverse effects of climate change. Climate adaptation strategies are actions and policies designed to minimize the negative impacts of climate change while enhancing resilience across ecosystems, economies, and communities. Unlike mitigation, which focuses on reducing greenhouse gas emissions, adaptation prepares systems to cope with current and future climate risks, such as disaster risk reduction (DRR). Risk reduction focuses specifically on implementing measures to minimize the detrimental impacts of flooding, including the construction of dams, the management of flood risk (Bekhira et al., 2019), the strategic operation of reservoirs, flood risk simulation, and the integration of green roofs for sustainable water management (Ayari et al., 2016; Aroua, 2020; Benslimane et al., 2020; Mezenner et al., 2022; Mehta et al., 2023; Bentalha, 2023; Zegait and Pizzo, 2023; Verma et al., 2023, Trivedi and Suryanarayana, 2023; Shaikh et al., 2024). For enhanced risk comprehension and management, it is advisable to conduct a thorough assessment and future projection of climate change impacts, with particular emphasis on arid and semi-arid regions (Choukrani et al., 2018).

The intensification of precipitation patterns driven by climate change could be perceived as beneficial, particularly for countries with arid or semi-arid climates, such as Egypt, where increased rainfall may help alleviate chronic water scarcity and enhance groundwater recharge (El Moukhayar et al., 2015; Chibane and Ali-Rahmani, 2015; Bemmoussat et al., 2017; Qureshi et al., 2024). However, this can lead to a marked increase in the frequency and severity of floods across many regions worldwide (Hafnaoui et al., 2022; Hafnaoui et al., 2023; Gassi and Saoudi, 2023). Warmer global temperatures intensify the hydrological cycle, causing more evaporation (Boutoutaou et al., 2020) and, consequently, heavier rainfall events (Boubakeur, 2018; Nassa et al., 2021). This surge in extreme precipitation overwhelms natural drainage systems and man-made infrastructure (Grasso, 2021). resulting in widespread urban flooding, riverine floods, and flash floods (Nashwan et al., 2019; Marzouk et al., 2021; Remini, 2023; Salem et al., 2024). Low-lying and densely populated regions are particularly vulnerable, facing devastating economic losses, displacement of communities, and long-term environmental degradation. As climate change accelerates, addressing the link between increased rainfall and flood risk becomes essential for global disaster preparedness and sustainable urban planning (Trenberth, 2011; Hountondji et al., 2019).

In Egypt, nearly all flash floods in recent years have occurred in the Sinai and Red Sea regions, which is why most flood studies and protection measures are concentrated in these areas. Likewise, floodwater harvesting techniques have been predominantly implemented in these regions (Bauer et al., 2020; El-Rawy et al., 2023; Ezz, 2017; Orabi, 2021; Ramadan et al., 2022). However, in October 2023, an unexpected reported flash flood struck Mersa Matruh, a city on Egypt's northern coast, resulting in significant infrastructure damage. This event underscores the increasing unpredictability of flash floods, even in areas not traditionally prone to such hazards (Abdelkareem and Mansour, 2023; Badir and AlRahman, 2017; Salem et al., 2024). These floods reflect the broader impacts of climate variability in arid and semi-arid regions, where changing precipitation patterns can lead to severe hydrological responses.

Due to the absence of runoff measurements across most Egyptian catchments, hydrological modeling plays a crucial role in flood analysis and risk assessment. Even in cases where measurement data are available, modeling remains essential for simulating flood scenarios, assessing potential risks, and planning mitigation strategies. However, the lack of observed data poses challenges for model calibration and validation. To address this, the study utilizes the SCS TR-55 method integrated with HEC-HMS, which is well-suited for regions with limited data availability due to its reliance on readily obtainable parameters such as land use and soil type (Mishra and Singh, 2013, El Bastawesy et al., 2019; Ezz, 2018; Nazirah et al., 2021).

Other methods, such as the Rational Method or SWAT (Soil and Water Assessment Tool), were considered. The Rational Method, while simple and effective for small catchments, is not suitable for the larger and more complex basins in this study. Similarly, while SWAT provides detailed watershed modeling, it requires extensive input data and calibration, which is impractical given the limited availability of long-term observations in the study area. The SCS TR-55 method was ultimately chosen because it balances practicality, robustness, and compatibility with the study objectives, making it an appropriate choice for this specific context. Its suitability has been demonstrated in multiple studies in Egypt, including applications in arid and semi-arid regions (El Bastawesy et al., 2019; Maher et al., 2022; Adbullah et al., 2023; ElBagoury and Gad, 2024, 2023; Hagras, 2023, Mahmoud et al., 2015). These studies validate its effectiveness in modeling runoff, managing flood risks, and adapting to regional hydrological conditions.

In addition, GIS environment plays a crucial role in several domains of hydraulic engineering, such as water resources management, hydrological exploration, predicting areas vulnerable to flood risk (Faregh and Benkhaled, 2016; Jaiswal et al., 2023; Deb, 2024). By integrating spatial data, GIS allows for the analysis of multiple factors, each with assigned weights to reflect their relative importance in flood susceptibility. Key factors include the elevation of the study area, slope gradients, land use and land cover (LULC), precipitation distribution patterns, and proximity to streams. Each of these factors contributes differently to flood risk, with lower elevations, steeper slopes, high precipitation areas, and proximity to streams typically indicating higher susceptibility. The combination of these weighted variables within the GIS framework allows for the creation of detailed flood risk maps, which are essential for flood management and mitigation planning (Tehrany et al., 2014; Ayari et al., 2016; Elsadek et al., 2018).

The previous hydrological studies in the Mersa Matruh region have primarily focused on quantifying water volumes generated by precipitation in various wadis and assessing their impact on the local water budget, as detailed by EL-Sabri et al. (2011). This particular study calculated runoff and groundwater recharge in five wadis north of Mersa Matruh, examining the role of groundwater recharge in mitigating seawater intrusion. Similarly, Sabet et al. (2017) investigated the hydrological potential of surface and groundwater recharge in Wadi El Sanab, one of the largest wadis in northern Mersa Matruh, with a focus on sustainable development for Bedouin communities and strategies for utilizing stored precipitation water. Another study by Abou Hussien et al. (2020) explored runoff harvesting in the El-Hraka basin, east of Mersa Matruh, aiming to secure water for

supplementary irrigation during dry months. This study employed stony dams and man-made underground storage galleries to facilitate runoff harvesting. Abdalla et al. (2021) conducted a similar study in Wadi Al Raml, northern Mersa Matruh, also aimed at runoff harvesting for agricultural use during non-rainy months. They recommended the construction of reservoirs to store runoff water. These studies consistently emphasize the conservation of runoff water for sustainable development, yet all are conducted in wadis located outside the area affected by the October 2023 event.

The objective of this study is to investigate the causes of the October 2023 flood in Mersa Matrouh, Egypt, through a comprehensive analysis of hydrological and geographical factors. This includes delineating the watershed of the study area using Geographic Information System (GIS) techniques to understand its hydrological characteristics. The study also examines the intensity and distribution of the rainfall event that triggered the flood and its contribution to the inundation. A flood risk assessment is conducted by developing a weighted overlay model that integrates key factors, including elevation, slope, land use and land cover, precipitation, and proximity to streams. The resulting flood risk map identifies high-risk zones and highlights their vulnerability to extreme hydrological events, providing critical insights for flood mitigation planning and risk management in the region.

STUDY AREA

Mersa Matruh, located on the Mediterranean coast of Egypt, is the capital of the Mersa Matruh Governorate. Positioned approximately 240 km west of Alexandria and around 220 km from the Egyptian-Libyan border, the city is renowned for its distinctive geographical and climatic conditions. Mersa Matruh is celebrated for its stunning beaches and historical significance, contributing to its unique regional character. The study area affected by the October 2023 flood is situated in the eastern region of Mersa Matruh. This area encompasses Wadi Al Raml, Al Kharrouba, and Kilo Four, as shown in Fig. 1.

This study represents the first comprehensive scientific investigation of a flood event in a coastal city along Egypt's southern Mediterranean coast, situated within a vulnerable semi-arid zone. The flood reported in October 2023, which marks the first catastrophic flood in the recorded history of Matruh Governorate, is unexpected and triggered by severe thunderstorms, associated with Storm Daniel, over the study area (Figure 2). Given the region's historical lack of significant flooding, this event underscores the increasing vulnerability of such zones to extreme weather phenomena, likely exacerbated by climate change.

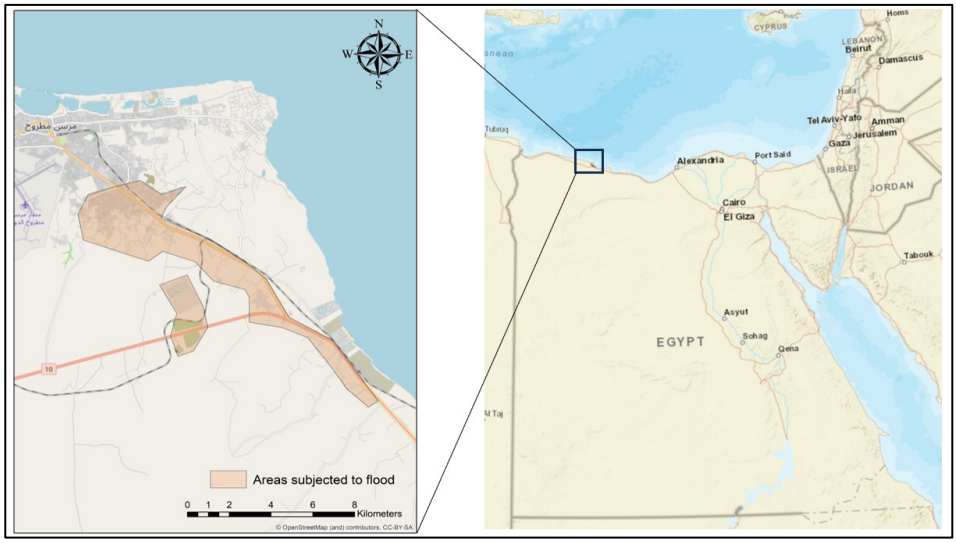

Figure 1

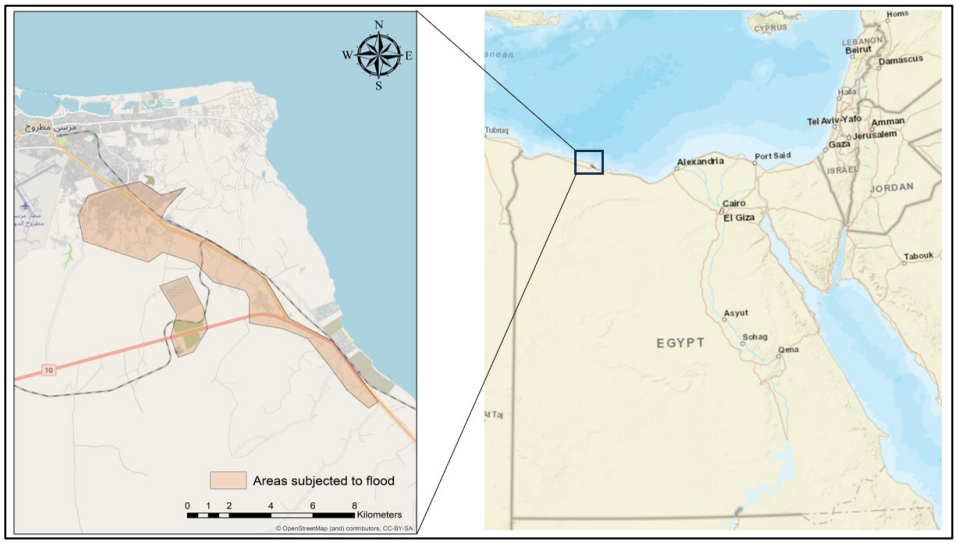

Figure 1: Areas subjected to October 2023 flood event

Figure 2: Real photos for the study area during the flood (5 October, 2023)

DATA USED

Digital Elevation Model

A Digital Elevation Model (DEM) provides a digital representation of the surface terrain within the study area. Constructed using GIS software from Shuttle Radar Topography Mission (SRTM) data with a 1-arc second grid spacing (30 meters), and projected to UTM WGS84 Zone 35N, this DEM offers a high-resolution basis suitable for hydrological analysis. The DEM is crucial for calculating topographic parameters necessary for watershed delineation, including basin slopes, slope lengths, and shape. Additionally, it plays a key role in estimating hydrologic parameters such as flow directions, flow accumulation, stream networks, and longest flow length, as illustrated in **Erreur ! Source du renvoi introuvable.**a.

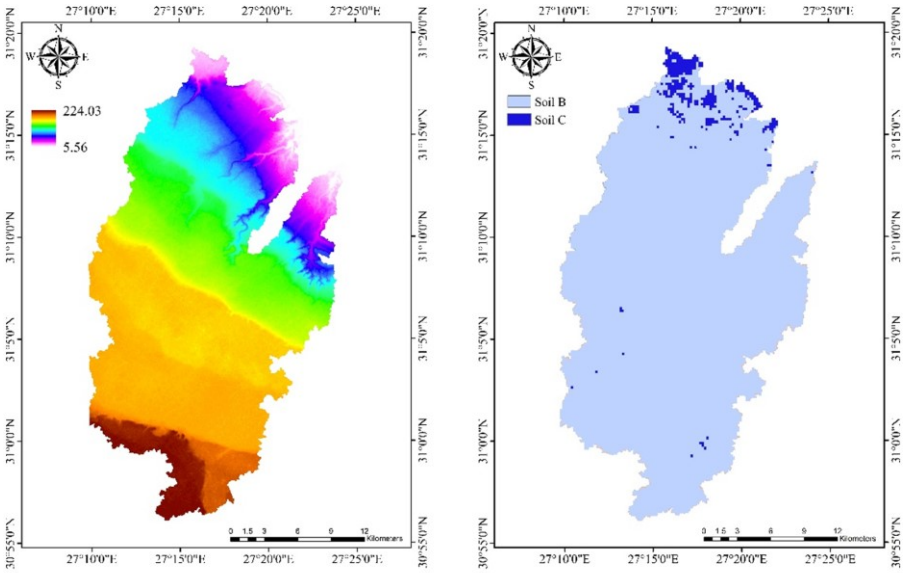

Figure 3: (a) Study area Digital Elevation Model in meters, and (b) Hydrological soil group

Hydrological Soil Groups

One of the key factors in the Soil Conservation Service (SCS) method is the determination of hydrological soil groups (HSG) as shown in **Erreur ! Source du renvoi introuvable.**b. These groups are classified into four categories: A, B, C, and D (Ross et al., 2018). Soils in Group A have the lowest runoff potential and the highest infiltration rates, making them ideal for reducing surface water accumulation. Group B soils exhibit moderate infiltration rates and a moderate potential for surface runoff. Group C soils, with lower infiltration rates, have a higher potential for runoff compared to Group B soils. Finally, Group D soils possess the highest runoff potential and the lowest infiltration rates. To model precipitation -runoff for the study area, a hydrological soil group map is clipped and integrated into a GIS environment to calculate the weighted average Curve Number (CN) which will be discussed later.

Precipitation Data Collection

Meteorological analysis forms a critical component of this study, as it serves as the foundational step for estimating precipitation depths and potential runoff quantities. A precipitation frequency analysis is essential to determine the expected precipitation depth for various return periods (probability of exceedance). For this purpose, precipitation data

is sourced from the U.S. National Climate Data Center's Global Summary of Days (GSOD) database (Nashwan et al., 2019). Rain gauges in the vicinity of the study area are evaluated, with the Mersa Matruh rain gauge (WMO ID 623060) providing the most significant contributions. Long-term precipitation records from this station, spanning 24 years (2000–2023), are utilized. These records cover a spatial zone with a 50 km radius and include daily precipitation depth measurements. From this dataset, the maximum annual precipitation depth for each year is calculated, as illustrated in Figure 4.

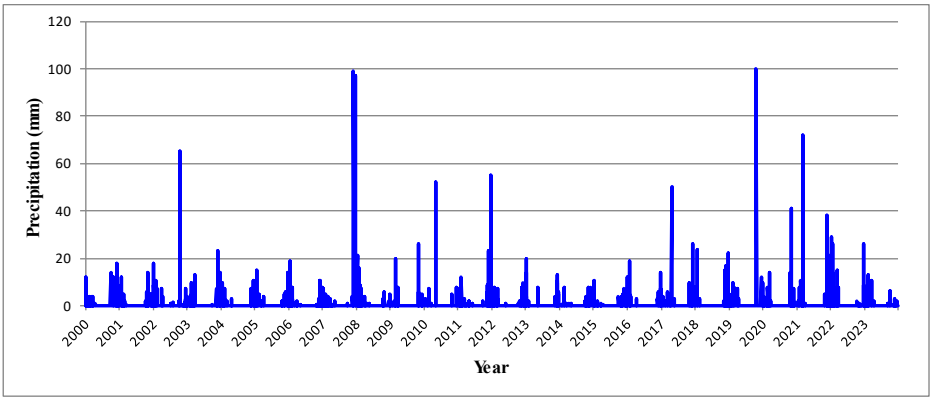

Figure 4: Daily Precipitation (2000 – 2023)- Mersa Martuh Rain Gauge

The graph shows daily precipitation data for Mersa Matruh, Egypt, a semi-arid, from 2000 to 2023. Precipitation is periodic, with notable peaks indicating occasional heavy precipitation events typical of coastal areas. The data shows long periods of minimal precipitation, consistent with the semi-arid climate, where most rain occurs during the cooler months, typically from October to February. These patterns highlight the region's vulnerability to both droughts and flash floods, necessitating careful water resource management and infrastructure planning.

Land use and cover

Land use and land cover (LULC) play a crucial role in determining the runoff potential. In this study, the LULC map of the study area is developed using high-resolution data sourced from the Environmental Systems Research Institute (ESRI), a globally recognized provider of reliable GIS-based spatial data Venter et al. (2022). The map categorizes the area into six distinct land cover classes: water bodies, trees, crops, rangeland, bare ground, and built-up areas. These categories are illustrated in Figure 5, which provides a spatial overview of the study area.

The area covered by each LULC class has been calculated and it is found that the largest portion of the study area is rangeland, covering approximately 556.34 km² (91.17% of the total area). This is followed by bare ground, which accounts for 47.65 km² (7.81%). Built-up areas, representing urbanized zones, make up 4.94 km² (0.81%). Other classes,

including water bodies (0.8 km², 0.13%), trees (0.446 km², 0.07%), and crops (0.0399 km², 0.01%), occupy smaller proportions of the region.

This analysis highlights the significant influence of rangeland and bare ground, which dominate the study area, on runoff potential. Additionally, the presence of built-up areas contributes to increased impervious surfaces, intensifying surface runoff during storm events. The integration of this detailed LULC data into the hydrological model enhances the precision of flood risk assessment and supports the development of effective flood mitigation strategies.

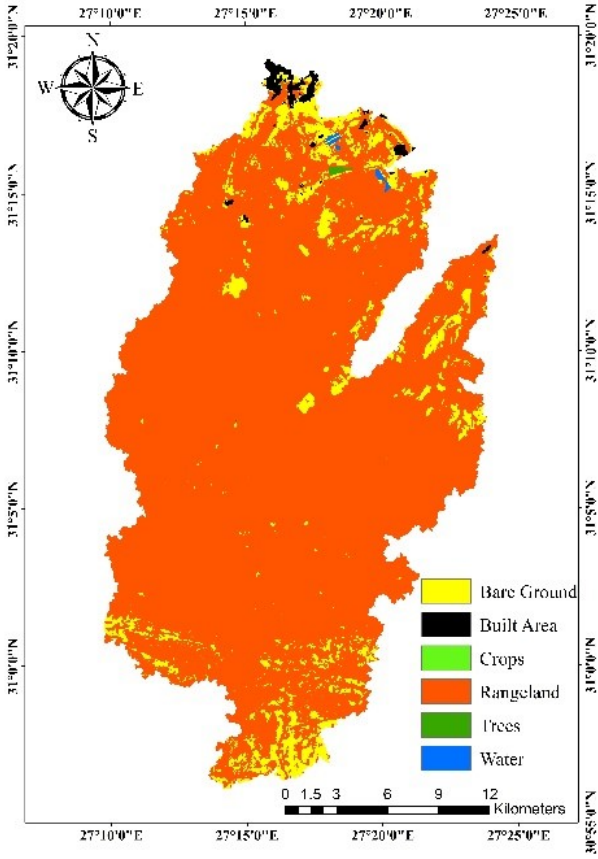

Figure 5: The Land Use / Land Cover (LULC) of the study area

EXPLORING THE CAUSES BEHIND THE OCTOBER 2023 FLOOD

This section aims to explain the flooding incident that occurred in Mersa Matruh in October 2023. After collecting the precipitation records for the past 24 years (2000–2023), it is evident that the recorded precipitation depth that triggered the flood is

relatively small —only 6.5 mm, significantly lower than the recorded precipitation depths occurred in many other occasions without any recorded flooding of the study area. This raises an important question: why did the study area experience flooding from such a minor event, despite the absence of any previous flood records in recent decades? The region has been subjected to larger precipitation events exceeding 100 mm in the past without any recorded flooding. This study seeks to explore potential hypothetical reasons for the unexpected flood event and provides a concise justification for selecting a 50-year return period precipitation event for modeling. This return period is commonly used in flood protection planning due to its practicality and balance between extreme event analysis and design feasibility.

Contributing Factors to the October 2023 Flood: Several hypothetical factors may have contributed to the flooding incident:

1. **Potential Inaccuracy in Recorded Precipitation Data**: The recorded precipitation depth on October 5, 2023, was only 6.5 mm, which is unusually small to cause significant flooding. It is possible that this value underrepresents the actual precipitation due to limitations in the measurement equipment or localized variations in rainfall intensity that were not captured by the monitoring station.
2. **Inadequate or Malfunctioning Drainage Infrastructure**: The flood may have resulted from insufficient maintenance or failure of existing drainage systems, which were unable to manage even minor precipitation events.
3. **Urbanization Effects**: Increased impervious surfaces due to urban development could have intensified surface runoff, overwhelming the drainage capacity.
4. **Antecedent Soil Moisture Conditions**: Elevated soil moisture levels prior to the rainfall event could have reduced infiltration capacity, leading to higher surface runoff.
5. **Topographical and Land Use Changes**: Changes in the region's topography or land use over time may have exacerbated vulnerability to flooding.

The purpose of this section is not to confirm specific causes of the October 2023 flood but rather to raise critical questions and propose plausible factors that might have influenced the event. Future studies involving detailed field investigations, improved monitoring, and advanced hydrological modeling are necessary to validate these hypotheses and refine the understanding of flood dynamics in the region.

In addition to exploring potential hypothetical causes, this study also identifies areas at high risk of future flooding and estimates runoff discharge and volumes for the basins in the study area using a 50-year return period precipitation event. This return period, commonly used in flood protection planning, provides a practical benchmark for evaluating hydrological responses. These findings are intended to guide future research and inform the development of effective flood management strategies to mitigate risks and enhance resilience.

METHODOLOGY

All the aforementioned datasets are processed to derive the necessary variables for estimating runoff quantities. The first step involved conducting watershed delineation in the area impacted by the October 2023 flood. Following this, precipitation data underwent statistical analysis to determine the appropriate precipitation depth for various return periods, facilitating runoff estimation.

Watershed Delineation

The watershed delineation for the study area is performed using ArcMap 10 GIS software. Morphological parameters essential for hydrological analysis are calculated using the Hydrology Tool in ArcGIS, utilizing a 1-arc second DEM. These parameters include catchment boundaries, filling sinks, flow direction, flow accumulation, and the main stream network. Figure 6 illustrates the basins and main streamlines generated in ArcGIS after defining five outlets that correspond to the flooded areas during the October storm event. The total drainage area of the five basins contributing runoff to the study area is approximately 600 km². The delineated streams are compared with satellite imagery from Google Earth, demonstrating a good match.

Table 1 provides details on the areas, average slopes, longest flow path lengths, and drainage density for each basin.

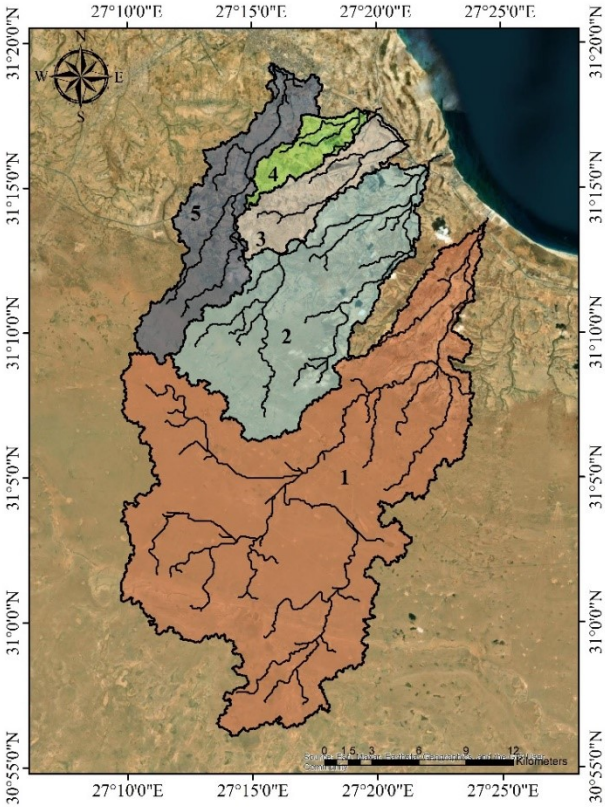

Figure 6: Results of Delineation of the study area; subbasins and identified streams

Table 1: Study area basins characteristics

Basin Name	Area (km^2)	Slope (%)	Longest Flow path (km)	Drainage Density (Km/Km^2)
Basin – 1	356.12	2.2	62.30	0.54
Basin – 2	135.03	2.7	32.69	0.66
Basin – 3	29.24	2.2	16.92	0.62
Basin – 4	20.33	2.3	16.24	0.87
Basin – 5	56.72	2.1	27.30	0.72

Precipitation Data Analysis

Mersa Matruh is a coastal city situated on the Mediterranean Sea, characterized by a warm, humid, and clear summer, while winters are cold, windy, and mostly clear. Like much of Egypt, Mersa Matruh falls within an arid climate zone, with generally low annual precipitation. However, the city is prone to occasional heavy precipitation events, particularly during the winter months. The rainy season typically spans from September to March, making the region vulnerable to sudden downpours and flash floods during this period.

Using the daily precipitation data from the Mersa Matruh station, the maximum precipitation event for each year is first calculated to represent the most significant precipitation occurrences annually. These maximum values are then subjected to flood frequency analysis using the Log-Pearson III distribution method. This approach allows for the estimation of precipitation depths associated with various return periods, such as 2, 5, 10, 25, 50, and 100 years as shown in Table 2. The results of the analysis provide critical insight into the potential for extreme precipitation events and their expected magnitude.

Table 2: Flood frequency analysis by Log-Pearson III distribution method

Return Period (Years)	Probability (%)	Precipitation (mm)
2	50	24.54
5	20	47.01
10	10	67.06
25	4	96.55
50	2	122.66
100	1	149.84

RESULTS

In this study, the Soil Conservation Service Curve Number (SCS-CN) method is employed to estimate surface runoff for the delineated watersheds. The curve number (CN) is calculated based on preprocessed land use, soil, and hydrological data, providing a foundation for predicting runoff. Using the HEC-HMS software, surface runoff calculations are performed to estimate the runoff discharge generated by a 50-year return period storm. Subsequently, a flood hazard map is developed to identify areas at high risk of flooding, enabling focused attention on these vulnerable regions for future flood protection planning.

CN selection

The runoff curve number (CN) is a key empirical parameter in the SCS method for estimating surface runoff and infiltration from precipitation excess. The CN value is determined based on the area's hydrologic soil group and land use characteristics. It ranges from 0 to 100, where higher values indicate greater surface runoff, while lower values suggest higher soil infiltration and less runoff. According to the SCS TR-55, the CN values for natural desert areas are 63, 77, 85, and 88 for hydrological soil groups A, B, C, and D, respectively. To calculate an equivalent CN for each delineated basin in the study area, a weighted average method is applied. This approach ensures that the varying characteristics of different land types and soil groups within each basin are accurately reflected in the overall CN value. This involves using equation (1), which accounts for the percentage of the total area corresponding to each CN:

$$\mathrm{CN}_{\mathrm{weighted}} = \sum_{i=1}^{n} \left(\frac{\mathrm{Area}_i}{\mathrm{Total\ Area}} \times \mathrm{CN}_i \right) \quad (1)$$

Where CN_i refers to the CN value for the portion of the basin with an area A_i, this equation allows for the calculation of a representative curve number that accounts for the land use and hydrologic soil group characteristics of each basin segment. Ultimately, the equivalent ($CN_{weighted}$) values for the five delineated basins are found to be 77.01, 77.07, 77.71, 78.68, and 78.00, respectively as shown in Table 3. These values reflect the varying runoff potential across the different watersheds contributing to the October 2023 flood event in Mersa Matruh.

Table 3: $CN_{weighted}$ calculation for the 5 basins of the study area

Basin	HSG	Area (km^2)	CN	$CN_{weighted}$
1	B	355.46	77	77.01
	C	0.43	85	
2	B	133.24	77	77.07
	C	1.23	85	
3	B	30.32	77	77.71
	C	2.95	85	
4	B	14.15	77	78.68
	C	3.76	85	
5	B	56.62	77	78.00
	C	8.12	85	

The weighted Curve Number ($CN_{weighted}$) was calculated based on the Hydrological Soil Group (HSG) for each delineated basin. While Land Use/Land Cover (LULC) data typically play a role in CN estimation, it was determined that bareground and rangeland collectively account for approximately 99% of the study area. Consequently, the impact

of other LULC categories on runoff characteristics is negligible. Therefore, the CN values used for this study are derived primarily from the HSG classification, ensuring that the methodology remains representative of the dominant landscape features within the region.

Surface Runoff Calculation

The Hydrologic Engineering Center's Hydrologic Modeling System (HEC-HMS) is a widely utilized tool for simulating precipitation-runoff processes. Developed by the US Army Corps of Engineers Hydrologic Engineering Center, HEC-HMS software is designed to model hydrological processes in basins by integrating spatial and temporal elements of dendritic watershed systems (Choudhari et al., 2014; Tassew et al., 2019; Ben Said et al., 2024). The model is extensively used in hydrological studies to simulate both short-term and long-term runoff events, enhancing the understanding of hydrological processes and water availability. HEC-HMS employs the SCS method to estimate runoff quantities, incorporating key basin characteristics such as area, slope, weighted CN, time of concentration, infiltration, initial interception, stream length, and precipitation depth. The Soil Conservation Service (SCS) TR-55 method is widely recognized for its applicability in ungauged catchments, particularly in arid and semi-arid regions, due to its reliance on land use, soil type, and hydrological conditions. Its suitability for the Mersa Matruh study area is supported by previous studies (El Bastawesy et al., 2019; Nazirah et al., 2021).

In this study, HEC-HMS is used to predict flood hydrographs based on these variables, utilizing a hypothetical storm event Type II. The SCS Type II rainfall distribution was used to represent the hypothetical storm event for this study. This distribution is well-suited for regions experiencing intense, short-duration rainfall events, which are characteristic of arid and semi-arid climates. Studies such as Soulis et al. (2021) and others have validated its effectiveness in simulating precipitation patterns typical of Mediterranean-like environments. Incorporating this distribution ensures that the modeling approach aligns with regional hydrological characteristics and established methodologies.

The Muskingum routing method was employed in the HEC-HMS model to simulate flow within the channel networks. This method was selected due to its effectiveness in handling flood wave movement in natural channels. The time of concentration for each basin was estimated using the Kirpich equation.

The HEC-HMS software is utilized to simulate the runoff quantities for the five studied basins, incorporating their unique characteristics and a precipitation depth corresponding to a 50-year return period. This precipitation event, commonly used in flood protection, is selected to evaluate the basins' ability to manage extreme precipitation. The simulation aimed to assess the runoff response under these conditions.

The graph illustrated in Figure 7 represents the relation between runoff discharge and time for the five basins. Basin 1 exhibits the highest peak discharge, followed by Basin 2, Basin 5, Basin 3, and Basin 4. The runoff increases sharply after approximately 14

hours, reaching a peak before gradually decreasing as the flow recedes. The differences in the peak discharge and timing between basins can be attributed to variations in basin characteristics, such as size, slope, and infiltration rates, which influence the rate of water collection and release. These results provide critical insights into the basins' hydrological response under extreme precipitation conditions. Detailed data for the runoff discharge, volume of water and time to peak are presented in Table 4.

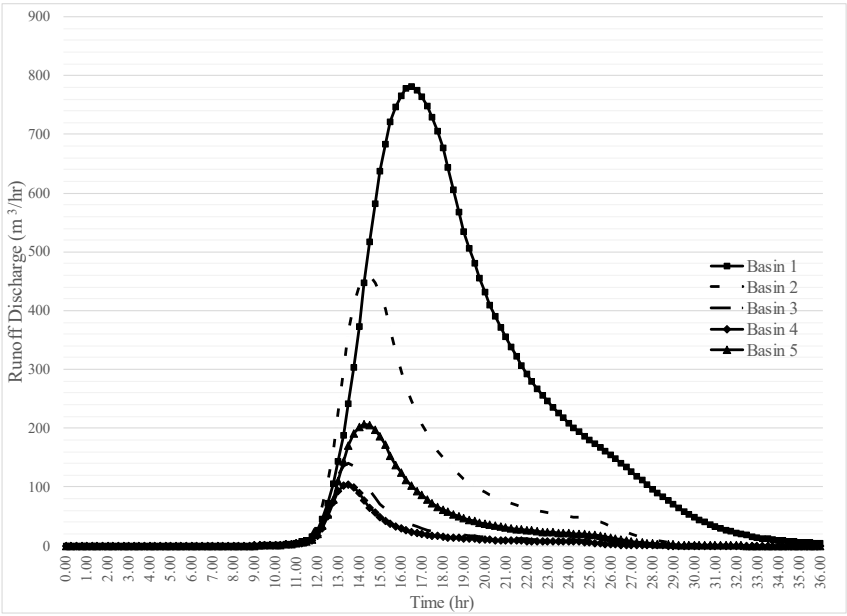

Figure 7: Runoff hydrograph for the five basins for a 50-year return period event

Table 4: Calculated runoff details for the five basins

	Peak Runoff (m^3/s)	Time to peak (hr)	Volume (1000 m^3)
Basin – 1	782.3	16.50	22414.0
Basin – 2	460.4	14.50	8534.8
Basin – 3	139.6	13.50	1894.0
Basin – 4	103.7	13.50	1359.8
Basin – 5	206.7	14.25	3701.1

The peak runoff discharge, time to peak, and total runoff volume are analyzed for each basin. Basin 1 exhibited the highest peak runoff discharge at 782.3 m^3/s, with a time to peak of 16.5 hours and a total runoff volume of 22,414,000 m^3. Basin 2 followed with a peak discharge of 460.4 m^3/s, peaking at 14.5 hours and contributing a total runoff volume

of 8,534,800 m³. Basins 3, 4, and 5 showed lower peak discharges, with Basin 3 reaching 139.6 m³/s and a time to peak of 13.5 hours, Basin 4 with 103.7 m³/s and a similar time to peak of 13.5 hours, and Basin 5 at 206.7 m³/s peaking at 14.25 hours. The corresponding total runoff volumes for these basins are 1,894,000 m³, 1,359,800 m³, and 3,701,100 m³, respectively. These values highlight the variation in runoff response across the basins due to their distinct hydrological and topographical characteristics.

Flood Hazard Map

Flood hazard assessment studies are crucial for mitigating potential damage from extreme weather events. In this study, the morphometric characteristics of the delineated watersheds have been analyzed to estimate, demonstrate, and assess the flood risk in the affected area. A comprehensive flood hazard map is illustrated, highlighting the varying degrees of risk. This map serves as a foundational tool for flood mitigation efforts and urban planning, providing valuable insights for future risk management and infrastructure development in this region.

The flood risk map developed in this study is based on several critical factors: elevation, slope, land use/cover, proximity to streams, and precipitation. Other factors can be considered but, in this study, these are the only factors are concerned. Each factor of those is reclassified into five categories according to its probability to flood as follows:

Elevation

The study area is classified into five flood risk categories: very low, low, moderate, high, and very high. Areas of very low and low flood risk are predominantly located in the central and southern portions of the study area, which likely feature higher elevations. These elevated regions facilitate natural water drainage, reducing the likelihood of surface water pooling or flood accumulation. The higher terrain also acts as a natural barrier against surface runoff, further decreasing flood vulnerability. In summary, there is a clear inverse relationship between elevation and flood risk—the higher the elevation, the lower the risk of flooding.

Slope

Similarly, the study area slopes are classified into five categories based on their gradient: slopes between 0–2% are considered very high risk, 2–5% as high risk, 5–10% as moderate risk, 10–20% as low risk, and slopes greater than 20% as very low risk. This classification mirrors the pattern observed with elevation—areas with steeper slopes tend to have a lower flood risk. Steeper slopes facilitate quicker surface water runoff, minimizing the accumulation of water and reducing flood hazards. Therefore, the higher the slope, the lower the flooding risk in the area.

Land use/cover

Water bodies and agricultural lands near streams and flat regions significantly contribute to increased flood risk. These areas typically have less permeable surfaces, which can intensify runoff and hinder water infiltration. The lack of permeable ground allows water to accumulate rapidly, leading to higher surface runoff. Furthermore, inadequate urban planning and the absence of sufficient drainage infrastructure can exacerbate this vulnerability, heightening the potential for flooding in these regions. Effective flood management strategies are thus essential to mitigate these risks.

Proximity to streams

A proximity to streams map is generated and classified, to the same five categories, to highlight areas at varying levels of flood risk based on their distance from natural drainage networks such as streams, and wadis. The hydrologic analysis shows that high-risk zones are predominantly concentrated around these features, indicating that proximity to streams plays a critical role in flood vulnerability. This underscores the importance of stream proximity in flood events, particularly during periods of heavy precipitation.

Precipitation

The precipitation data used in this study is obtained from the WorldClim 2.1 database (Fick and Hijmans, 2017). This database provides global spatially interpolated monthly climate data at a very high spatial resolution (1 km²). To focus on the study area, the precipitation data is clipped to the study area. Since the records are on a monthly basis, the highest values for the same month across the study area are selected. Similar to the other flood risk factors, this data is reclassified, with areas receiving higher precipitation classified as having a higher flood risk.

The five mentioned factors are classified as mentioned and conducted using ArcGIS software as illustrated in Figure 8.

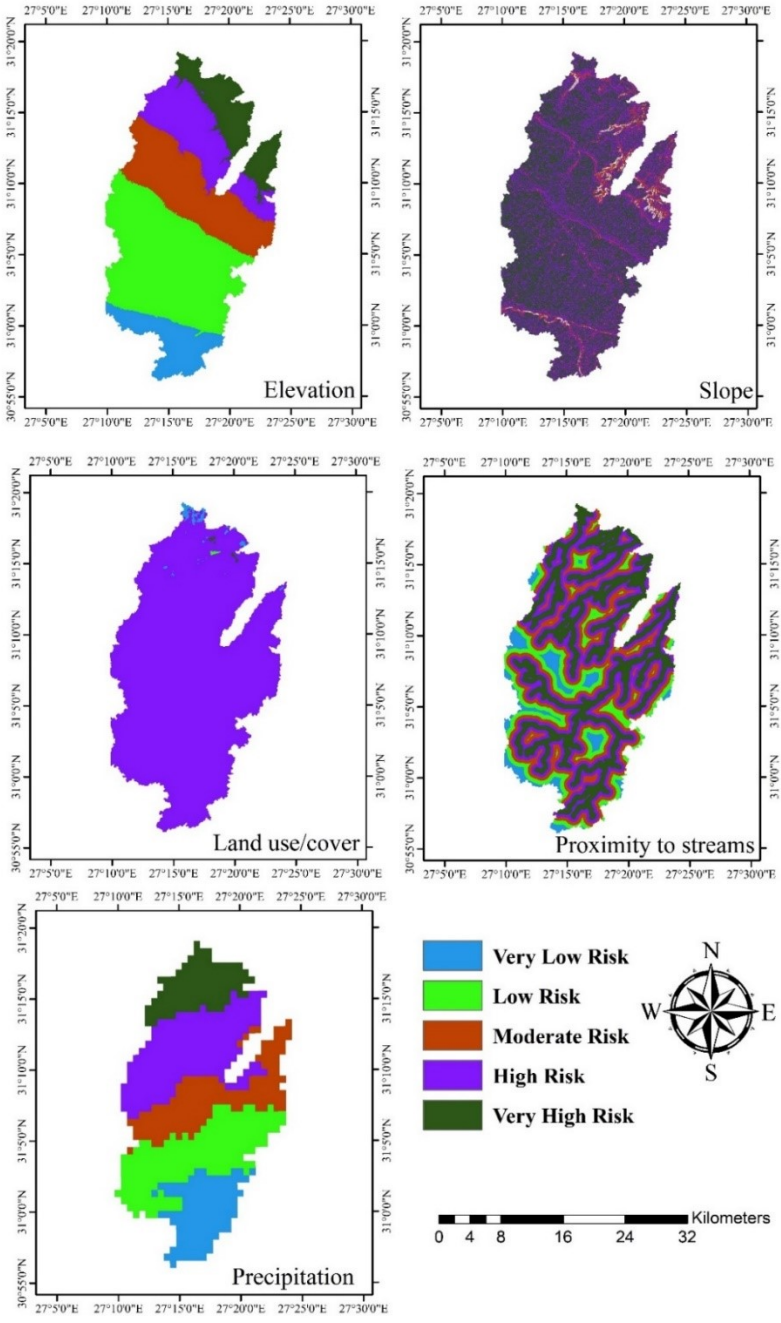

Figure 8: The five classified factors used to generate a flood hazard maps

After generating the classified maps for the various factors, each factor is assigned a specific weight based on its relative contribution to flood risk (Alharbi, 2024). The assigned weights for elevation, slope, land use/cover, proximity to streams, and precipitation are 10%, 15%, 10%, 30%, and 35%, respectively.

The weights assigned to the flood-inducing factors are derived from a review of existing studies that assess flood susceptibility in arid and semi-arid regions. Precipitation (35%) and proximity to streams (30%) are assigned the highest weights, consistent with their critical roles in flood generation (e.g., Alharbi, 2024; Elsadek et al., 2018). Slope (15%) and elevation (10%) are given moderate weights due to their influence on runoff velocity and accumulation, as supported by Tehrany et al. (2014). Finally, land use/cover (10%) was considered less impactful in this context, given the predominance of natural rangeland and bare ground in the study area (El Bastawesy et al., 2019).

These weighted factors are then integrated using ArcGIS software to create a composite flood risk map. The map categorizes the study area into five distinct flood risk levels: Very Low Risk, Low Risk, Medium Risk, High Risk, and Very High Risk as illustrated in Figure 9. This classification provides a valuable tool for visualizing flood-prone areas, supporting future flood management and mitigation efforts.

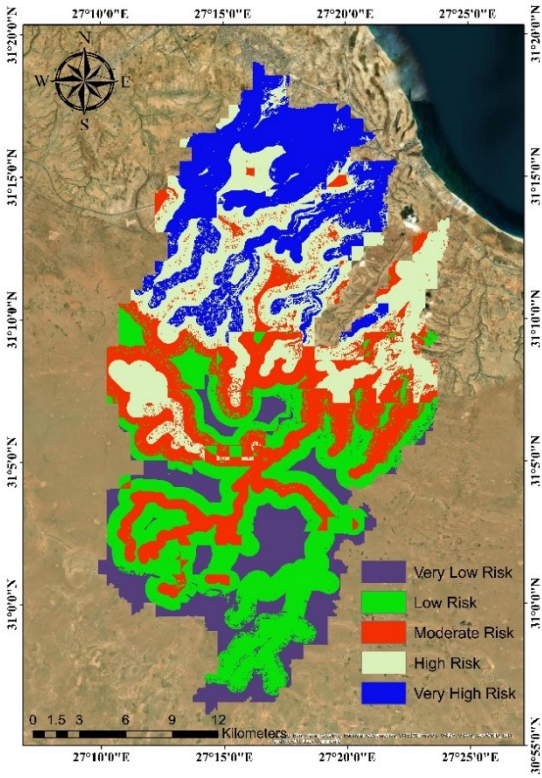

Figure 9: Flood Hazard Map

DISCUSSION

Precipitation Data Assessment

As illustrated in Figure 4, the maximum daily precipitation recorded is 100.8 mm on 23th October, 2019, while the minimum daily precipitation is 0.3 mm on various dates throughout the period. Analysis of the data indicates that October to December typically experience the highest precipitation events in Mersa Matruh. These months show a higher frequency of significant precipitation, which aligns with the flooding observed in October 2023. This seasonal pattern suggests that the region is particularly susceptible to intense precipitation and potential flooding during the autumn months.

After calculating the flood frequency analysis, it is notable that the flood in Mersa Matruh in October 5th, 2023 occurred with a recorded precipitation depth of only 6.5 mm, which is surprisingly lower than the calculated precipitation depth for even the 2-year return period (24.54 mm).

Given the flood event reported in the study area on October 5th, 2023, it is observed that the precipitation depth on that day is even lower than that of a 2-year return period storm. This raises uncertainty as to why flooding occurred, especially since the area has experienced higher precipitation depths in the past without any recorded flooding. To address this, the study proceeded by calculating the surface runoff generated by a 50-year return period storm and subsequently developing a flood hazard map. These results aim to support future efforts in designing effective flood protection strategies for the area.

Surface Runoff Analysis

The runoff analysis is conducted using the HEC-HMS software (Mehta and Yadav, 2024; Kherde et al., 2024), simulating the hydrological response of the five basins under a 50-year return period precipitation event, which is typically used depth for selecting the best flood protection technique (Figure 7). The simulation results highlight distinct differences in the runoff behavior of each basin, reflecting the varying physical characteristics such as basin size, slope, land cover, and drainage efficiency.

The peak runoff discharge also varied significantly among the basins, with larger basins generally producing higher discharge rates. This suggests that catchment area plays a critical role in determining the volume of runoff that can accumulate during a precipitation event.

The time to peak for the basins showed considerable variation, with some basins responding more quickly to the precipitation event, while others exhibited a slightly delayed response. This variability is likely due to differences in size and topography. Basins that reached their peak runoff discharge earlier in the simulation are more prone to flash flooding due to their rapid response to precipitation, and they may require prompt intervention during storm events. In contrast, basins with a slower runoff response might experience prolonged flooding, making them susceptible to sustained water accumulation over time. These differences underline the need for tailored flood protection strategies for

each basin, ensuring that areas with faster runoff are equipped with quick drainage solutions, while those with higher runoff volumes can handle prolonged inundation.

This analysis provides critical insights into the hydrological responses of the basins, forming the basis for further studies aimed at designing flood protection measures for the study area. The results from the HEC-HMS simulation will guide future efforts to mitigate flood risks and enhance the resilience of the region to extreme precipitation events.

Flood Hazard Assessment

The flood hazard map, illustrated in Figure 9, categorizes the study area into five distinct flood risk zones: Very Low Risk, Low Risk, Moderate Risk, High Risk, and Very High Risk. This classification is based on a weighted assessment of critical flood-inducing factors, including elevation (10%), slope (10%), land use/cover (10%), proximity to streams (30%), and precipitation (35%). Each factor is chosen for its significant impact on flood vulnerability. Proximity to streams and precipitation carry the highest weight due to their direct influence on flood occurrence, while elevation, slope, and land use/cover provide additional refinement to the flood susceptibility model.

The areas classified as Very High Risk (blue) are particularly vulnerable to flooding. These zones are concentrated in the northern and eastern parts of the study area, which feature low-lying terrain and proximity to streams, making them prone to slow water runoff and accumulation. These regions coincide with the actual flooding event that occurred in October 2023, further validating the model's accuracy. The prediction of flood-prone zones is essential for proactive flood management, as it helps prioritize areas requiring the most attention for flood mitigation measures.

The High-Risk zones (beige) follow a similar spatial pattern to the very high-risk areas, located near streams and also at lower elevations. Though not as vulnerable as the very high-risk areas, they still require significant flood protection strategies, especially during periods of intense precipitation. Without intervention, these areas could experience recurrent flooding, with severe implications for infrastructure, agriculture, and local communities.

Moderate Risk areas (red) are mostly transitional zones, where moderate slopes and elevations contribute to a mix of both high runoff and some retention of water. These areas, though less prone to consistent flooding, are still at risk, particularly during extreme weather events or sudden increases in precipitation. In these zones, floodproofing infrastructure, such as reinforcing buildings and developing emergency response systems, could mitigate potential damages.

In contrast, Low Risk areas (green) and Very Low Risk areas (purple) are generally situated in higher elevations and steeper slopes in the southern parts of the study area. These regions naturally drain water more effectively, reducing the likelihood of prolonged flooding. However, despite their relative safety, the increasing unpredictability of climate events necessitates ongoing monitoring to ensure that these areas remain safe,

particularly under extreme precipitation conditions that could shift local hydrological patterns.

The map's real-world validation, highlighted by the October 2023 flood, underscores the critical importance of addressing the very high and high-risk zones. In these areas, the most effective flood mitigation strategies could include enhancing drainage systems, constructing flood barriers (dikes or dams), and developing early warning systems. These measures are essential to protect lives, reduce economic losses, and maintain infrastructure resilience. Additionally, land use regulations in these high-risk zones should be strictly enforced to prevent further development in flood-prone areas, which could exacerbate the flood hazard. For moderate-risk areas, localized floodproofing—such as raised buildings, permeable surfaces to enhance water infiltration, and improved stormwater management systems—can reduce flood exposure. Education and preparedness campaigns could also be launched to raise awareness in these areas about flood risk and how to respond during a flood event. Finally, looking at low and very low-risk areas, while these zones are currently less affected by flooding, it is crucial not to ignore them. Long-term planning should consider the potential impact of climate change, which could increase precipitation intensity and frequency, shifting flood risks in the future. This map serves as a foundational tool for urban planners and disaster management agencies to devise climate-resilient infrastructure plans.

In conclusion, this flood hazard map provides a comprehensive, scientifically grounded view of the study area's flood risk. The areas most susceptible to flooding—validated by the October 2023 flood event—should be the focus of immediate mitigation efforts. Urban planning, infrastructure development, and community preparedness should prioritize these zones to reduce the future impact of floods. The lower-risk zones, while safer, should still be monitored and prepared for potential changes in risk due to evolving weather patterns. Future versions of the model could incorporate climate change data, soil properties, and groundwater levels to further refine risk predictions.

CONCLUSION

This research addresses the unexpected flood event in Mersa Matruh in October 2023, which occurred despite a relatively low rainfall depth compared to previous storms. The study applied a systematic approach combining hydrological modeling, remote sensing, and GIS-based tools to assess the flood dynamics. The analysis is carried out using the Soil Conservation Service Curve Number (SCS-CN) method for runoff calculations, followed by surface runoff simulations using HEC-HMS for a 50-year return period storm.

The results indicated significant variability in the hydrological response across the five delineated basins, with Basin 1 displaying the highest peak runoff discharge (782.3 m^3/s) and Basin 4 showing the lowest (103.7m^3/s). Time to peak also varied, ranging from 13.5 to 16.5 hours across the basins. A flood hazard map is also generated to highlight high-risk areas for future flood events, integrating environmental factors such as elevation, slope, and proximity to streams.

The findings suggest that inadequate or poorly maintained flood protection infrastructure, combined with the area's topographical characteristics, may have contributed to the flooding. This study emphasizes the need for more robust flood protection strategies, particularly in vulnerable areas, to mitigate future flood risks. The insights gained from this research provide a basis for future flood management planning, helping to safeguard the region against similar flood events.

Further research is strongly recommended to identify and evaluate optimal flood protection strategies and their strategic implementation locations. This recommendation is particularly critical given the anticipated impacts of climate change and the projected increase in precipitation intensity along Egypt's northern coast. Such studies will be instrumental in ensuring the region's future resilience against flood events and in developing adaptive management strategies that account for evolving climatic conditions.

Declaration of competing interest

The author declares that he has no known competing financial interests or personal relationships that could have appeared to influence the work reported in this paper.

REFERENCES

ABDALLA M.A.I., WAHAB M.K.A.E., TAWFIK M.A., KHATER I.M.M. (2021). Application of Hydrological Models in a Small Agricultural Catchment for Water Management: Case Study on Wadi El-Raml Watershed-North Western Coast of Egypt, Plant Archives, Vol. 21, No. 2, pp. 154–163. https://doi.org/10.51470/plantarchives.2021.v21.no2.026

ABDELKAREEM M., MANSOUR A.M. (2023). Risk assessment and management of vulnerable areas to flash flood hazards in arid regions using remote sensing and GIS-based knowledge-driven techniques, Natural Hazards, Vol. 117, No. 3, pp. 2269–2295. https://doi.org/10.1007/s11069-023-05942-x

ABOU HUSSIEN E., ISMAIL M., OMRAN W., ABOU ALFOTOH M. (2020). Water Harvesting For Sustainable Development of El-Hraka Basin in the North-western Coast of Egypt, Egyptian Journal of Soil Science, Vol. 60, No. 3, pp. 263–376. https://doi.org/10.21608/ejss.2020.31570.1361

ALHARBI T. (2024). A Weighted Overlay Analysis for Assessing Urban Flood Risks in Arid Lands: A Case Study of Riyadh, Saudi Arabia, Water, Vol. 16, No. 3, pp. 1-14. https://doi.org/10.3390/w16030397

ARGAZ A. (2018). 1d model application for integrated water resources planning and evaluation: case study of Souss river basin, Morocco, Larhyss Journal, No 36, pp. 217-229.

AROUA N. (2018). Water resources in SNAT 2030. between economic needs and ecological requirements, Larhyss Journal, No 35, pp. 153-168. (In French)

AROUA N. (2020). Flood risk reduction strategy in Algiers a brief modern history (XVIthC -XIXthC), Larhyss Journal, No 43, pp. 73-89.

AROUA N. (2023). Setting out urban water issues examples from Algeria and worldwide, Larhyss Journal, No 56, pp. 309-327.

AYARI K., DJEBBI M., CHAKROUN H. (2016). Flood risk mapping of the city of El Bab Medjez by the overflow of the Medjerda, Larhyss Journal, No 25, pp. 285-307. (In French)

BADIR M.K., ALRAHMAN H.A. (2017). Climate Change and Extreme Events over Dabaa Region, Egypt, Climate Change Research at Universities: Addressing the Mitigation and Adaptation Challenges, pp. 263–273. https://doi.org/10.1007/978-3-319-58214-6_16

BAUER F., HADIDI A., TÜGEL F., HINKELMANN R. (2020). Flash Flood Investigations in El Gouna, Northern Red Sea Governorate, Flash Floods in Egypt, pp. 61–81. https://doi.org/10.1007/978-3-030-29635-3_5

BEKHIRA A., HABI M., MORSLI B. (2019). The management of flood risk and development of watercourses in urban areas: case of the town of Bechar, Larhyss Journal, No 37, pp. 75-92. (In French)

BEN SAID M., HAFNAOUI M.A., HACHEMI A., MADI M., BENMALEK A. (2024). Evaluating the Effectiveness of the Existing Flood Risk Protection Measures Along Wadi Deffa in El-Bayadh City, Algeria, Larhyss Journal, No. 59, pp. 7–28.

BENSLIMANE M., BERREKSI A., BENMAMAR S., BOUACH A. (2020). Flood risk numerical simulation of Bejaia city urban zone (Algeria), Larhyss Journal, No 42, pp. 167-178.

BENTALHA C. (2023). Evaluation of the hydraulic and hydrology performance of the green roof by using SWMM, Larhyss Journal, No 53, pp. 61-72.

BEMMOUSSAT A., ADJIM M., BENSAOULA F (2017). Use of the ZYGOS model for the estimation of groundwater recharge in Sikkak watershed (Northen west of Algeria), Larhyss Journal, No 30, pp. 105-119. (In French)

BOUBAKEUR G. (2018). Climatic drought in the semi-arid region of Djelfa –Algeria (analyses of the rainfall data from 1975 to 2016), Larhyss Journal, No 33, pp. 123-140.

BOUGUERRA S.A., BENSLIMANE N. (2017). Characterization of drought weather in climate semiarid: case of watershed wadi Boumessaoud (N-W Algeria), Larhyss Journal, No 29, pp. 95-110. (In French)

BOUTOUTAOU D., ZEGGANE H., SAGGAI S. (2020). Evaporation from the water surface of lakes and reservoirs of the arid zone of the mediterranean: case of Algeria, Larhyss Journal, No 43, pp. 91-101.

CHADEE A., NARRA M., MEHTA D., ANDREW J., AZAMATHULLA H. (2023). Impact of climate change on water resource engineering in Trinidad and Tobago, Larhyss Journal, No 55, pp. 215-229.

CHIBANE B., ALI-RAHMANI S.E. (2015). Hydrological based model to estimate groundwater recharge, real- evapotranspiration and runoff in semi-arid area, Larhyss Journal, No 23, pp. 231-242.

CHOUDHARI K., PANIGRAHI B., PAUL J.C. (2014). Simulation of rainfall-runoff process using HEC-HMS model for Balijore Nala watershed, Odisha, India, International Journal of Geomatics and Geosciences, Vol. 5, No. 2, pp. 253–265.

CHOUKRANI G., HAMIMSA A., SAIDI M.E., BABQIQI A. (2018). Diagnosis and future projection of climate change in arid zone. case of Marrakech-Safi region (Morocco), Larhyss Journal, No 36, pp. 49-63. (In French)

DEB S. (2024). Optimizing hydrological exploration through GIS-based groundwater potential zoning in Gomati district, Tripura, India, Larhyss Journal, No 60, pp. 231-256.

EL MOUKHAYAR R., BAHIR M., CARREIRA P. (2015). Estimation of groundwater recharge in arid region through hydrochemistry and isotope: a case study Kourimat basin Morocco, Larhyss Journal, No 23, pp. 87-104.

EL-RAWY M., ELSADEK W.M., DE SMEDT F. (2023). Flood hazard assessment and mitigation using a multi-criteria approach in the Sinai Peninsula, Egypt, Natural Hazards, Vol. 115, No. 1, pp. 215–236. https://doi.org/10.1007/s11069-022-05551-0

EL-SABRI M.A., MASOUD M.H., DAHAB K.A. (2011). Water budget assessment for some Wadis West Mersa Matrouh and possibilities of sea water intrusion, Journal of the Sedimentological Society of Egypt, Vol. 19, pp. 113–125.

El-BAGOURY H., GAD, A. (2024). Integrated hydrological modeling for watershed analysis, flood prediction, and mitigation using meteorological and morphometric data, SCS-CN, HEC-HMS/RAS, and QGIS. Water, Vol. 16, No. 2, pp. 1–20.

EL BASTAWESY M., ATTWA M., ABDEL HAFEEZ T.H., GAD A. (2019). Flash floods and groundwater evaluation for the non-gauged dryland catchment using remote sensing, GIS and DC resistivity data: A case study from the Eastern Desert of Egypt, Journal of African Earth Sciences, Vol. 152, pp. 245–255. https://doi.org/10.1016/j.jafrearsci.2019.02.004

ELSADEK W.M., IBRAHIM M.G., MAHMOD W.E. (2018). Flash Flood Risk Estimation of Wadi Qena Watershed, Egypt Using GIS Based Morphometric Analysis, Applied Environmental Research, Vol. 40, No. 1, pp. 36–45. https://doi.org/10.35762/aer.2018.40.1.4.

EZZ H. (2017). The utilization of GIS in revealing the reasons behind flooding Ras Gharib City, Egypt, International Journal of Engineering Research in Africa, Vol. 31, pp. 135–142. https://doi.org/10.4028/www.scientific.net/JERA.31.135

EZZ H. (2018). Integrating GIS and HEC-RAS to model Assiut plateau runoff, Egyptian Journal of Remote Sensing and Space Science, Vol. 21, No. 3, pp. 219–227. https://doi.org/10.1016/j.ejrs.2017.11.002

FAREGH W., BENKHALED A. (2016). GIS based SCS-CN method for estimating runoff in Sigus watershed, Larhyss Journal, No 27, pp. 257-276. (In French)

FICK S.E., HIJMANS R.J. (2017). WorldClim 2: new 1-km spatial resolution climate surfaces for global land areas, International Journal of Climatology, Vol. 37, No. 12, pp. 4302–4315. https://doi.org/10.1002/joc.5086

GASSI K.A.A., SAOUDI H. (2023). The effect of the physical parameterization schemes in WRF-ARW on the quality of the prediction of heavy rains that cause flooding application on eastern Algeria, Larhyss Journal, No 56, pp. 123-137.

GRASSO V. (2021). 2020 State of Climate Services report: Risk Information and Early Warning Systems, EGU General Assembly Conference Abstracts, Paper ID EGU21–74.

HAFNAOUI M.A., MADI M., BEN SAID M., BENMALEK A. (2022). Floods in El Bayadh city: causes and factors, Larhyss Journal, No 51, pp. 97-113.

HAFNAOUI M.A., BOULTIF M., DABANLI I. (2023). Floods in Algeria: analyzes and statistics, Larhyss Journal, No 56, pp. 351-369.

HAGRAS, A. (2023). Runoff modeling using SCS-CN and GIS approach in the Tayiba Valley Basin, Abu Zenima area, South-west Sinai, Egypt. Modeling Earth Systems and Environment,Vol. 9, No. 4, pp. 3883–3895.

HOUNTONDJI B., CODO F.P., DAHOUNTO S.V.H., GBAGUIDI T.B. (2019). Flood management in urban environment: case of the Cotonou city in Benin, Larhyss Journal, No 39, pp. 333-347. (In French)

JAISWAL T., JHARIYA D., SINGH S. (2023). Identification and mapping of groundwater potential zone using analytical hierarchy process and GIS in lower Kharun basin, Chhattisgarh, India, Larhyss Journal, No 53, pp. 117-143.

KHERDE R.V., MEHTA D.J., MORE K.C., SAWANT P.H. (2024). Dynamic watershed modelling: HEC-HMS analysis of a tropical watershed, Larhyss Journal, No 60, pp. 87-111.

MEHTA D., ACHOUR B., PASTAGIA J., AZAMATHULLA H., VERMA S. (2023). Review of reservoir operation, Larhyss Journal, No 56, pp. 193-214.

MEHTA D., YADAV S. (2024). Rainfall runoff modelling using HEC-HMS model: case study of Purna river basin, Larhyss Journal, No 59, pp. 101-118.

MAHER M., NASRALLAH T., RABAH M., ABDELHALEEM F. (2022). Watershed Delineation and Runoff Estimation of Wadi Tayyibah, South Sinai Using Arc-GIS And HEC-HMS Model, Port-Said Engineering Research Journal, Vol. 26, No. 2, pp. 61 - 71. https://doi.org/10.21608/pserj.2022.111930.1155

MAHMOUD S. H., ALAZBA A. A., ADAMOWSKI J., EL-GINDY A. M. (2015). GIS methods for sustainable stormwater harvesting and storage using remote sensing for land cover data-location assessment. Environmental monitoring and assessment, Vol. 187, pp. 1-19.

MARZOUK M., ATTIA K., AZAB S. (2021). Assessment of Coastal Vulnerability to Climate Change Impacts using GIS and Remote Sensing: A Case Study of Al-Alamein New City, Journal of Cleaner Production, Vol. 290, pp. 1-19. https://doi.org/10.1016/j.jclepro.2020.125723

MEZENNER N., BENKACI T., BERMAD A., DECHEMI N. (2022). Dam reservoir operation optimization using genetic algorithm and principal component analysis simulation model - case of dam Ghrib reservoir, Larhyss Journal, No 51, pp. 145-160.

MISHRA S.K., SINGH V.P. (2013). Soil Conservation Service Curve Number (SCS-CN) Methodology, Springer Science and Business Media, Vol. 42.

NAKOU T.R., SENOU L., ELEGBEDE B., CODO F.P. (2023). Climate variability and its impact on water resources in the lower mono river valley in Benin from 1960 to 2018, Larhyss Journal, No 56, pp. 215-234.

NASSA R.A.K., KOUASSI A.M., BOSSA S.J. (2021). Analysis of climate change impact on the statistical adjustment models of extreme rainfall case of Ivory Coast, Larhyss Journal, No 46, pp. 21-48.

NASHWAN M.S., SHAHID S., WANG X. (2019). Assessment of satellite-based precipitation measurement products over the hot desert climate of Egypt, Remote Sensing, Vol. 11, No. 5, pp. 555. https://doi.org/10.3390/rs11050555

NAZIRAH A., SABKI W.O. W.M., ZULKARNIAN H., AFIZAH A. (2021). Simulation of runoff using HEC-HMS for ungauged catchment, AIP Conference Proceedings, Vol. 2347, No 1. https://doi.org/10.1063/5.0051957

NICHANE M., KHELIL M.A. (2015). Climate change and water resources in Algeria - vulnerability, impact and adaptation strategy, Larhyss Journal, No 21, pp. 25-33. (In French).

ORABI O. (2021). Flash Flood Risk in West-Central Sinai, Egypt, Egyptian Journal of Geology, 65(1), 137–154. https://doi.org/10.21608/egjg.2021.101672.1008

QURESHI H.U., ABBAS I., SHAH S.M.H., TEO F.Y. (2024). Hydrologic evaluation of monthly and annual groundwater recharge dynamics for a sustainable groundwater resources management in Quetta city, Pakistan, Larhyss Journal, No 60, pp. 27-53.

RAMADAN E.M., SHAHIN H.A., ABD-ELHAMID H.F., ZELENAKOVA M., ELDEEB H.M. (2022). Evaluation and Mitigation of Flash Flood Risks in Arid Regions: A Case Study of Wadi Sudr in Egypt, Water, Vol. 14, No. 19, Paper ID 2945. https://doi.org/10.3390/w14192945

REMINI B. (2020). Algeria: the climate is changing, the water is becoming scarce, what to do? Larhyss Journal, No 41, pp. 181-221. (In French)

REMINI B. (2023). Flash floods in Algeria, Larhyss Journal, No 56, pp. 267-307.

ROSS C.W., PRIHODKO L., ANCHANG J., KUMAR S., JI W., HANAN N.P. (2018). HYSOGs250m, global gridded hydrologic soil groups for curve-number-based runoff modeling, Scientific Data, Vol. 5, No. 1, pp. 1-9. https://doi.org/10.1038/sdata.2018.91

SABET H.S., ISMAIL Y.L., F HAWASH S.A., EL DEEN E.S. (2017). Hydrology of Wadi El Sanab, El Qasr area, West Mersa Matrouh, Northwestern Coastal Zone-Egypt, International Journal of Innovative Science, Engineering and Technology, Vol. 4, No 3, pp. 171–191.

SHAIKH A.F., BHIRUD Y.L., MORE S.B., PAWAR A.D., VAIDYA O.V. (2024). Comparative analysis of optimization algorithms for reservoir operations: a case study on Ukai dam, Larhyss Journal, No 58, pp. 179-196.

SALEM H.M., ABDALLA M. A.I., METWALLY K.A. (2024). Assessment the impacts of land cover and climate changes on rainwater harvesting systems using remote sensing and runoff model in some Wadis of West Matrouh – Egypt, HydroResearch, Vol. 7, pp. 301–314. https://doi.org/10.1016/j.hydres.2024.05.002

SOULIS K.X. (2021). Soil conservation service curve number (SCS-CN) Method: Current applications, remaining challenges, and future perspectives. Water, Vol. 13, No 2, pp. 1-4.

TASSEW B.G., BELETE M. A., MIEGEL K. (2019). Application of HEC-HMS Model for Flow Simulation in the Lake Tana Basin: The Case of Gilgel Abay Catchment, Upper Blue Nile Basin, Ethiopia, Hydrology, Vol. 6, No. 1, Paper ID 21. https://doi.org/10.3390/hydrology6010021

TEHRANY M.S., PRADHAN B., JEBUR M.N. (2014). Flood susceptibility mapping using a novel ensemble weights-of-evidence and support vector machine models in GIS, Journal of Hydrology, Vol. 512, pp. 332–343. https://doi.org/10.1016/j.jhydrol.2014.03.008

TORRESAN S., CRITTO A., DALLA VALLE M., HARVEY N., MARCOMINI A. (2008). Assessing coastal vulnerability to climate change: comparing segmentation at global and regional scales, Sustainability Science, Vol. 3, No 1, pp. 45–65. https://doi.org/10.1007/s11625-008-0045-1

TRENBERTH K. (2011). Changes in precipitation with climate change, Climate Research, Vol. 47, No. 1, pp. 123–138. https://doi.org/10.3354/cr00953

TRIVEDI M., SURYANARAYANA T.M.V. (2023). An assessment of optimal operation policies for a reservoir using particle swarm optimization, Larhyss Journal, No 56, pp. 107-121.

VERMA S., SAHU R.T., PRASAD A.D., VERMA M.K. (2023). Reservoir operation optimization using ant colony optimization a case study of Mahanadi reservoir project complex Chhattisgarh – India, Larhyss Journal, No 53, pp. 73-93.

ZEGAIT R., PIZZO H.S. (2023). Flood control reservoir using VBA simulation case of Idles basin in southern Algeria, Larhyss Journal, No 53, pp. 41-60.